Ground- and Excited-State Properties of DNA Base Molecules from Plane-Wave Calculations Using Ultrasoft Pseudopotentials

M. PREUSS, W. G. SCHMIDT, K. SEINO, J. FURTHMÜLLER, F. BECHSTEDT
Friedrich-Schiller-Universität, Institut für Festkörpertheorie und Theoretische Optik, Max-Wien-Platz 1, 07743 Jena, Germany

Received 14 March 2003; Accepted 9 June 2003

Abstract: We present equilibrium geometries, vibrational modes, dipole moments, ionization energies, electron affinities, and optical absorption spectra of the DNA base molecules adenine, thymine, guanine, and cytosine calculated from *first principles.* The comparison of our results with experimental data and results obtained by using quantum chemistry methods show that in specific cases gradient-corrected density-functional theory (DFT-GGA) calculations using ultrasoft pseudopotentials and a plane-wave basis may be a numerically efficient and accurate alternative to methods employing localized orbitals for the expansion of the electron wave functions.

 J Comput Chem 25: 112–122, 2004

Key words: DFT-GGA calculations; ultrasoft pseudopotentials; adenine; thymine; guanine; cytosine; atomic structure; ionization energy; electron affinity; optical absorption

Introduction

Chemical simulation methods to study deoxyribonucleic acid (DNA) and its base molecules range from empirical molecular dynamics to *ab initio* quantum chemistry (see, e.g., refs. 1–3). The latter methods can be very accurate. Due to their unfavorable scaling properties, however, wave function-based methods such as Hartree–Fock or Møller–Plesset are restricted to systems containing relatively few atoms. Moreover, the application of a basis set consisting of a finite number of localized atom-centered functions leads to an inherent inaccuracy known as the basis set superposition error (BSSE). Controversies still exist with regard to the validity of counterpoise correction schemes[4] that are designed to correct for the BSSE (see, e.g., ref. 5). Furthermore, the usage of a necessarily incomplete basis of localized functions such as Gaussians for the expansion of the molecular electron wave functions renders the efficient and reliable control of the numerical convergence difficult. These problems do not exist if, instead, plane waves are used for the expansion of the electron wave functions. The straightforward implementation of periodic boundary conditions, important for the accurate calculation of extended systems, such as the interaction of molecules with crystal surfaces, is a further advantage of using plane waves for electronic structure calculations. Moreover, there exist theoretically well-founded schemes based on DFT plane-wave implementations that allow for a systematic improvement of the description of the electronic many-body effects in the excited states over the local density approximation (LDA)[6] or the generalized gradient approximation (GGA)[7,8] to the exchange and correlation potential. This concerns both the inclusion of electronic self-energy effects for the accurate description of unoccupied electronic states within the GW method[9–11] and the Bethe–Salpeter equation (BSE) for pair excitations to account for electron-hole attraction contributions to the optical response.[12–16] In contrast to time-dependent density-functional theory (TDDFT), GW and BSE-based approaches yield reliable results for both localized and extended systems.[17,18]

Indeed, DFT calculations using a plane-wave basis set were recently performed for DNA base pairs,[19] various assemblages of guanine molecules,[20] and the nucleotide crystal d(GpCpGpCpGpCpGpCpGpCpGpCp).[21] A serious drawback of plane-wave–based methods for molecular electronic structure calculations, however, consists in the high number of basis functions needed to obtain results that are numerically converged. This holds in particular for organic and biomolecules containing elements of the first row of the periodic table such as carbon, nitrogen, and oxygen.

In the present work we investigate the applicability of DFT–GGA in conjunction with a plane-wave basis and ultrasoft non-norm-conserving pseudopotentials[22] to the DNA bases. We show that by using ultrasoft pseudopotentials accurate and numerically converged molecular structures can be obtained with a relatively low energy cutoff for the plane-wave expansion. The approach is

Correspondence to: W. G. Schmidt; e-mail: wgs@ifto.physik.uni-jena.de

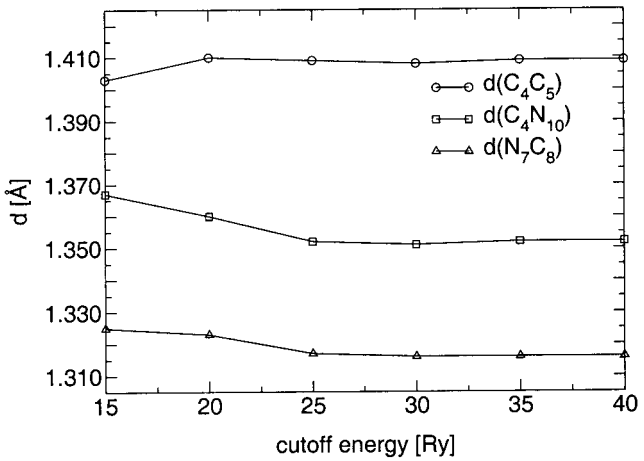

Figure 1. Equilibrium bond lengths (cf. Fig. 2) of gas-phase adenine vs. the plane-wave cutoff energy.

then applied to study the vibrational as well as electronic and optical properties of the base molecules, where relatively little and/or contradicting information is available from experiment and previous theoretical works. Thus, a wide range of ground- and excited-state properties of the DNA bases is calculated using one and the same numerically converged *ab initio* method.

Method

The total-energy and electronic-structure calculations are performed using the Vienna Ab-initio Simulation Package (VASP) implementation[23] of the gradient-corrected (PW91)[7] density functional theory. The electron-ion interaction is described by non-norm-conserving ultrasoft pseudopotentials,[22] allowing for the accurate quantum-mechanical treatment of first-row elements already with a low cutoff energy. The execution time of major parts of the code scales with the number of atoms N like $\mathcal{O}(N^2)$. The orthogonalization of the wave functions and the subspace diagonalization scale like $\mathcal{O}(N^3)$. Their contribution to the overall execution time, however, becomes dominant only for systems containing more than about 10^3 atoms. This favorable scaling behavior has allowed for modeling semiconductor structures containing nearly 3000 atoms using VASP.[24]

We performed extensive convergence tests on gas-phase adenine using a $10 \times 20 \times 20$ Å^3 supercell. The total energy and characteristic bond lengths are found to be completely converged (and the latter in excellent agreement with the experiment, cf. Fig. 1) if the electronic wave functions are expanded into plane waves up to a kinetic energy of 35 Ry. This constitutes a major computational saving, compared to the cutoff energy of 70 Ry found necessary in calculations using norm-conserving pseudopotentials.[19,21] For adenine, cytosine, and guanine (thymine) the cutoff of 35 Ry corresponds to a basis set of roughly 45,000 (94,000) plane waves. This still relatively high number results from the requirement to also "describe" the large vacuum region of the supercell. Therefore, the favorable scaling properties of the VASP implementation (compared to the scaling worse than $\mathcal{O}(N^4)$ for post-Hartree–Fock methods[25]) do not necessarily translate into a short execution time for systems such as studied here. A typical electronic relaxation using preconverged wave functions, such as occurring during structural relaxations or for calculations of vibrational modes, usually takes about 15 min on 32 processors of the Hitachi SR8000-F1.

As can be seen from Figure 1, the energy cutoff can be further reduced to 25 Ry, on the expense of a slightly increased error bar. We use the value of 35 Ry throughout the calculations. In the case of thymine, the size of the supercell had to be increased to $20 \times 20 \times 20$ Å^3.

Our calculations employ the residual minimization method–direct inversion in the iterative subspace (RMM-DIIS) algorithm[26,27] to minimize the total energy of the system. The molecular atomic structure is considered to be in equilibrium when the Hellmann–Feynman forces are smaller than 10 meV/Å. No symmetry constraints were applied during the structure optimization.

Results and Discussion

Geometries

Calculated bond lengths and bond angles for the most stable tautomers of the DNA bases, i.e., the keto-forms shown in Figure 2, are compiled in Tables 1 and 2, respectively. They are compared with high-resolution X-ray and neutron diffraction data summarized in a statistical survey of the Cambridge Structural Database by Clowney et al. (see ref. 28). The standard deviations in the samples amount to less than 0.002 Å for the bond lengths and less than 0.1° for the bond angles. The calculated values and the cited experimental findings agree within an error bar of typically less than 1–2%. A slight overestimation of bond lengths of this order of magnitude is to be expected for DFT-GGA calculations.[29] The bond lengths and bond angles of DNA base molecules have also

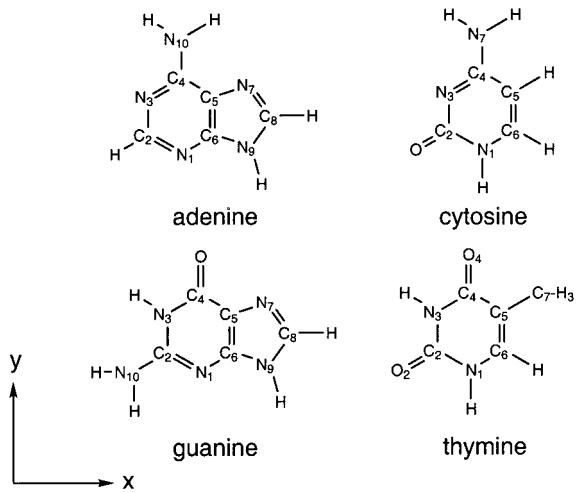

Figure 2. Schematic structures of most stable tautomers of the DNA bases.

Table 1. Calculated Bond Lengths (in Å) for Adenine, Cytosine, Guanine, and Thymine.

Adenine				Cytosine			
Bond	DFT-GGA	Ref. 33	Exp.	Bond	DFT-GGA	Ref. 30	Exp.
N_1C_2	1.341	1.333	1.331	N_1C_2	1.429	1.418	1.399
C_2N_3	1.348	1.342	1.339	C_2O	1.231	1.226	1.237
N_3C_4	1.350	1.342	1.351	C_2N_3	1.367	1.382	1.356
C_4N_{10}	1.352	1.353	1.335	N_3C_4	1.324	1.318	1.334
C_4C_5	1.409	1.409	1.406	C_4N_7	1.359	1.369	1.337
C_5C_6	1.396	1.396	1.383	C_4C_5	1.435	1.437	1.426
C_6N_1	1.339	1.336	1.344	C_5C_6	1.360	1.359	1.337
C_5N_7	1.383	1.385	1.388	C_6N_1	1.353	1.358	1.364
N_7C_8	1.316	1.308	1.311				
C_8N_9	1.381	1.380	1.373				
N_9C_6	1.381	1.377	1.374				
Guanine				**Thymine**			
Bond	DFT-GGA	Ref. 30	Exp.	Bond	DFT-GGA	Ref. 32	Exp.
N_1C_2	1.312	1.310	1.323	N_1C_2	1.389	1.366	1.376
C_2N_{10}	1.361	1.385	1.337	C_2O_2	1.227	1.218	1.220
C_2N_3	1.371	1.372	1.371	C_2N_3	1.383	1.368	1.373
N_3C_4	1.434	1.430	1.391	N_3C_4	1.406	1.384	1.382
C_4O	1.230	1.225	1.238	C_4O_4	1.233	1.218	1.228
C_4C_5	1.435	1.442	1.419	C_4C_5	1.459	1.461	1.445
C_5C_6	1.402	1.394	1.379	C_5C_6	1.354	1.329	1.339
C_6N_1	1.354	1.366	1.350	C_6N_1	1.376	1.380	1.378
C_5N_7	1.380	1.377	1.388	C_5C_7	1.495	1.498	1.496
N_7C_8	1.311	1.324	1.305				
C_8N_9	1.385	1.375	1.374				
N_9C_6	1.370	1.370	1.375				

Comparison is made with experimental data from ref. 28 and quantum-chemical results from refs. 30, 32, and 33.

been determined using a variety of quantum chemical methods such as MP2/6-31G(d,p),[30,31] HF/4-31G,[32] and B3LYP/6-311G(d,p) calculations.[33] The comparison of these predictions (also given in Tables 1 and 2) with the data presented here shows that plane-wave calculations using ultrasoft pseudopotentials are comparable in accuracy with those quantum-chemical approaches, at least concerning the bond lengths. Our results are also very close to those obtained in a recent DFT-GGA study using plane waves in conjunction with norm-conserving pseudopotentials.[20]

In contrast to the bond lengths, the planarity of the nucleic acid bases is still a somewhat open question (for a detailed discussion, see, e.g., refs. 34 and 35). It may have important consequences for the structure of DNA and molecular recognition processes. Originally believed to be perfectly planar, *ab initio* calculations carried out at the HF level with polarized basis sets of atomic orbitals suggest a weak nonplanarity of the amino groups of the base molecules.[36] More recent calculations indicate a rather strong amino group pyramidalization.[37–40] Clearly, the amount of pyramidalization depends strongly on the details of the calculations. For cytosine for example, Bludský et al.[41] obtain amino group hydrogen dihedral angles of 5.5 and 26.2°, using the HF/6-31G** and MP2/6-31G* levels of theory, respectively. The MP2/6-311G(2df,p) prediction, considered as benchmark, amounts to 21.4°. Our DFT-GGA calculations, in contrast, yield rather small deviations from planarity, cf. Table 3. In the case of cytosine, for example, a dihedral angle of 11.2° is found. The calculated nonplanarity of the other DNA base molecules is even smaller. It is interesting to note that similar to our results the DFT-GGA study by Di Felice et al.[20] also indicates a very weak nonplanarity.

The DFT-GGA approach thus seems not to be able to reproduce the order of NH_2 nonplanarity predicted by recent quantum chemistry calculations. This may be a consequence of the modeling of the exchange and correlation effects within DFT-GGA, which is exact only in the limit of the homogeneous electron gas. On the other hand, the structural consequences of rehybridization processes at solid surfaces, also characterized by strong charge inhomogeneities, are in general very reliably described in DFT calculations using either the LDA or the GGA to model exchange and correlation.[42,43] To probe the reliability of DFT-GGA in describing the nonplanarity of single molecules, we performed additional calculations for aniline ($C_6H_5NH_2$) for which experimental data on the nonplanarity are available. In this case we predict an out-of-plane angle of the amino group with respect to the ring plane of 34.0°, close to the value of 37.5° obtained by

Table 2. Calculated Bond Angles (in deg) for Adenine, Cytosine, Guanine, and Thymine.

Adenine				Cytosine			
Bond	DFT-GGA	Ref. 31	Exp.	Bond	DFT-GGA	Ref. 30	Exp.
$C_2N_3C_4$	117.6	118.3	118.6	$C_2N_3C_4$	120.7	119.9	119.9
$N_3C_2N_1$	128.9	128.9	129.3	$N_3C_2N_1$	115.9	115.9	119.2
$C_2N_1C_6$	111.7	110.8	110.6	N_3C_2O	125.9		121.9
$N_1C_6C_5$	126.1	127.1	126.8	N_1C_2O	118.2	118.9	118.9
$N_1C_6N_9$	129.5		127.4	$C_2N_1C_6$	123.4	124.0	120.3
$C_5C_6N_9$	104.4	104.3	105.8	$N_1C_6C_5$	120.0	119.6	121.0
$C_6C_5C_4$	116.5	116.0	117.0	$C_6C_5C_4$	116.2	116.0	117.4
$C_6C_5N_7$	111.6	112.0	110.7	$N_3C_4C_5$	123.7	124.6	121.9
$C_4C_5N_7$	131.8		132.3	$N_3C_4N_7$	116.8	116.8	118.0
$N_3C_4C_5$	119.1	118.9	117.7	$C_5C_4N_7$	119.4		120.2
$N_3C_4N_{10}$	120.9		118.6				
$C_5C_4N_{10}$	120.0	121.9	123.7				
$C_6N_9C_8$	106.8	106.9	105.8				
$N_9C_8N_7$	113.1	113.6	113.8				
$C_5N_7C_8$	104.1	103.2	103.9				
Guanine				Thymine			
Bond	DFT-GGA	Ref. 30	Exp.	Bond	DFT-GGA	Ref. 32	Exp.
$N_7C_8N_9$	112.5	112.9	113.1	$N_1C_2O_2$	123.3	123.1	123.1
$C_8N_7C_5$	105.0	103.8	104.3	$N_1C_2N_3$	112.4	113.6	114.6
$C_8N_9C_6$	106.9	106.9	106.4	$O_2C_2N_3$	124.3	123.3	122.3
$N_9C_6N_1$	125.5		126.0	$C_2N_1C_6$	123.7	123.4	121.3
$N_9C_6C_5$	105.0	104.8	105.4	$C_2N_3C_4$	128.3	127.4	127.2
$N_1C_6C_5$	129.4	129.5	128.6	$N_3C_4O_4$	120.2	120.4	119.9
$C_6N_1C_2$	112.2	111.5	111.9	$N_3C_4C_5$	114.7	115.2	115.2
$N_1C_2N_{10}$	120.6		119.9	$O_4C_4C_5$	125.2	124.4	124.9
$N_1C_2N_3$	123.2	124.1	123.9	$C_4C_5C_7$	118.5	117.8	119.0
$N_{10}C_2N_3$	116.2	115.9	116.2	$C_4C_5C_6$	117.9	117.9	118.0
$C_2N_3C_4$	127.2	127.0	125.1	$C_7C_5C_6$	123.6	124.3	122.9
N_3C_4O	118.5		119.9	$N_1C_6C_5$	123.0	122.5	123.7
$N_3C_4C_5$	109.2	108.9	111.5				
OC_4C_5	132.3	131.1	128.6				
$N_7C_5C_6$	110.6	111.6	110.8				
$N_7C_5C_4$	130.7		130.4				
$C_6C_5C_4$	118.7	118.9	118.8				

Comparison is made with experimental data from ref. 28 and quantum-chemical results from refs. 30–32.

microwave spectroscopy.[44] Unfortunately, there are no experimental data available on the amount of pyramidalization of gas-phase DNA bases.

Vibrational Modes

The relaxed geometries of cytosine and adenine are starting points for the calculation of their vibrational properties. The atoms of the molecules are treated as coupled three-dimensional harmonic oscillators. They are displaced away from their equilibrium positions, and the resulting Hellmann–Feynman forces are fitted to a quadratic equation in the distortion. The force constants resulting in the harmonic approximation are used to set up the dynamical matrix. The diagonalization of the dynamical matrix, finally, yields the vibrational frequencies and eigenmodes of the molecule.[45] Our results for cytosine and adenine are shown in Tables 4 and 5, respectively. The following notation has been chosen to classify the modes: ν—stretching (as: asymmetric, s: symmetric), β—bending or ring deformation (ro: rocking, sc: scissoring), γ—out-of-plane bending (to: torsional, $\gamma(\text{toNH}_{c/t})$: *cis*- resp. *trans*-H-atom), τ—ring deformation, inv: inversion, am: amino. As far as the modes can be clearcut classified, comparison is made with matrix-isolation experiments.[46,47]

In general, wavenumbers obtained theoretically and experimentally agree within 2–5% for the in-plane vibrational modes. This accuracy is comparable to *ab initio* frozen-phonon[45] or linear-response approach calculations for the dynamical properties of solid

Table 3. Dihedral Angles of the DNA Bases with Amino Group.

Base	Dihedral angle	rms Deviation from planarity[a]	
		C—NH_2 group	Molecule
Adenine	0.0°	0.000 Å	0.000 Å
Cytosine	11.2°	0.028 Å	0.020 Å
Guanine	2.3°	0.006 Å	0.023 Å

[a]With reference to a least-squares plane for the atoms of the dihedral group and for all atoms of the molecule, respectively.

surfaces.[48] Our results are less reliable for out-of-plane vibrations. This may be related to the nonharmonicity of the amino group vibrations:[41,49] The potential opposing the amino group rocking vibration is of a double-minimum character. Due to the coupling of the vibrational modes, inaccuracies in the description of the amino group modes will lead to perturbations of the complete spectrum. Nevertheless, the accuracy of the DFT-GGA calculations presented here is comparable to earlier MP2/6-31G(d,p) calculations for cytosine[50] and B3LYP/6-31G results for adenine.[46]

Dipole Moments

The electronic and optical properties of the DNA base molecules are less well understood than their structural details. The electrostatic potential around DNA bases is of primary importance for their molecular interactions, because it determines to a large extent not only their electrostatic interactions, but also the strength of H-bonding, hydration, and the bonding of small or polyvalent cations. Electronic ground-state properties such as molecular dipoles can be expected to be reliably described within DFT-GGA.

In the sense of a multipole expansion of the potential, the dipole moment describes the leading term contributing to the interactions and allows for a qualitative identification of binding sites. In Table 6 we compile the calculated dipole values for the DNA bases. Because of them being almost planar, we find the dipole moments perpendicular to the molecular planes (z-direction in Table 6) nearly negligible. In the case of adenine, we observe an excellent agreement with the experiment, while the DFT-GGA calculation seems to slightly overestimate the dipole moment of thymine. In the case of cytosine and guanine, the calculated values are smaller than measured. The DFT-GGA predictions are very close, however, to the results of quantum chemical calculations. The MP2/aug-cc-pVDZ values by Hobza and

Table 4. Calculated Eigenmodes and Eigenfrequencies (in cm^{-1}) of Cytosine.

No.	Mode	DFT-GGA	Exp.	No.	Mode	DFT-GGA	Exp.
1	$\nu(asNH_2)$	3817	3565	18	$\nu(N_1C_2)$	939	
2	$\nu(N_1H)$	3761			$\beta(R_1)$		
3	$\nu(sNH_2)$	3628	3441	19	$\gamma(C_6H)$	860	
4	$\nu(C_5H)$	3222			$\nu(N_1C_2)$	783	
5	$\nu(C_6H)$	3169			$\nu(C_4C_5)$		
6	$\nu(C_2O)$	1756	1720	21	$\gamma(C_5H)$	764	818
7	$\nu(C_5C_6)$	1664	1656		$\gamma(C_2O)$		
	$\nu(N_3C_4)$				$\tau(R_1)$		
8	$\beta(scNH_2)$	1550	1595	22	$\gamma(C_5H)$	763	781
9	$\nu(N_3C_4)$	1522	1539		$\gamma(C_2O)$		
	$\nu(C_4C_5)$			23	$\tau(R_1)$	690	
10	$\nu(N_3C_4)$	1443	1475		$\gamma(N_1H)$		
	$\nu(C_4N_{am})$			24	$\gamma(N_1H)$	697	637
	$\beta(C_5H)$			25	$\beta(R_2)$	605	614
	$\nu(C_6N_1)$			26	$\gamma(toNH_c)$	554	575
11	$\beta(N_1H)$	1403	1422		$\beta(R_2)$		
12	$\beta(C_6H)$	1292	1337	27	$\beta(R_2)$	513	537
	$\beta(C_5H)$			28	$\beta(C_2O)$	450	
	$\nu(C_4N_{am})$				$\gamma(toNH_c)$		
13	$\nu(C_2N_3)$	1261	1244		$\beta(C_4N_{am})$		
	$\nu(C_4N_{am})$			29	$\gamma(toNH_t)$	399	330
14	$\beta(C_6H)$	1169	1192		$\tau(R_3)$		
	$\beta(N_1H)$			30	$\tau(R_3)$	417	
	$\nu(C_6N_1)$			31	$\beta(C_4N_{am})$	265	260
	$\beta(C_5H)$				$\beta(C_2O)$		
15	$\beta(C_5H)$	1036		32	$\gamma(C_4N_{am})$	211	232
	$\nu(C_6N_1)$				$\gamma(C_2O)$		
16	$\beta(roNH_2)$	1003	1090	33	$\tau(R_2)$	161	197
17	$\beta(R_1)$	967			$\gamma(C_2O)$		
	$\nu(C_4C_5)$						

Comparison is made with experimental data from ref. 50.

Table 5. Calculated Eigenmodes and Eigenfrequencies (in cm^{-1}) of Adenine.

No.	Mode	DFT-GGA	Exp.	No.	Mode	DFT-GGA	Exp.
1	$\nu(asNH_2)$	3777	3557	22	$\beta(r_4)$	857	927
2	$\nu(N_9H)$	3760	3499		$\beta(r_5)$		
3	$\nu(sNH_2)$	3636	3442		$\nu(C_6C_5)$		
4	$\nu(C_8H)$	3332	3057	23	$\beta(R_1)$	851	869
5	$\nu(C_2H)$	2962	3041		$\beta(R_3)$		
6	$\beta(scNH_2)$	1758	1633	24	$\gamma(C_8H)$	799	848
	$\nu(C_6N_{10})$			25	$\tau(R_1)$	720	802
	$\nu(C_5C_6)$				$\tau(r_4)$		
7	$\nu(N_1C_6)$	1619	1606		$\gamma(C_6N_{10})$		
	$\nu(C_5C_6)$				$\gamma(C_8H)$		
8	$\beta(scNH_2)$	1597	1584	26	$\nu(N_1C_6)$	673	678
	$\nu(C_6C_5)$				$\beta(r_4)$		
9	$\nu(N_7C_8)$	1512	1482		$\nu(C_5N_7)$		
	$\beta(C_8H)$				$\nu(C_6N_9)$		
10	$\nu(C_6N_3)$	1472	1448	27	$\gamma(C_6N_{10})$	667	672
	$\beta(C_2H)$				$\tau(r_5)$		
	$\nu(C_6N_{10})$				$\tau(R_3)$		
	$\beta(scNH_2)$				$\tau(R_r)$		
	$\nu(C_2N_1)$			28	$\tau(r_4)$	641	655
11	$\nu(C_6C_5)$	1426	1419		$\tau(r_4)$		
	$\nu(C_6N_9)$			29	$\beta(r_5)$	619	610
12	$\beta(N_9H)$	1411	1374		$\nu(C_5C_6)$		
	$\beta(C_2H)$				$\beta(R_2)$		
	$\nu(C_8N_9)$			30	$\tau(R_2)$	594	566
	$\beta(R_1)$				$\gamma(N_9H)$		
13	$\nu(N_9C_8)$	1352	1340		$\tau(R_1)$		
	$\beta(C_8H)$				$\tau(r_5)$		
	$\beta(N_9H)$			31	$\beta(roNH_2)$	555	528
	$\nu(C_6N_3)$			32	$\beta(R_3)$	516	521
14	$\nu(N_3C_2)$	1332	1328		$\beta(R_2)$		
	$\nu(C_5N_7)$			33	$\gamma(N_9H)$	489	514
	$\beta(C_2H)$				$\tau(R_2)$		
15	$\nu(C_2N_1)$	1249	1268	34	$\beta(roNH_2)$	422	503
	$\nu(C_5N_7)$				$\beta(R_2)$		
	$\nu(N_3C_2)$				$\beta(C_6N_{10})$		
16	$\beta(C_8H)$	1223	1240	35	$\tau(R_3)$	295	298
	$\nu(N_7C_8)$				$\tau(r_5)$		
	$\beta(N_9H)$				$\tau(R_r)$		
17	$\beta(roNH_2)$	1124	1181		$\tau(R_2)$		
	$\nu(C_5N_7)$			36	$\beta(C_6N_{10})$	230	276
18	$\nu(C_6N_9)$	1050	1103		$\beta(R_2)$		
	$\beta(r_4)$			37	$\gamma(invNH_2)$	224	242
	$\nu(C_6N_{10})$				$\tau(R_r)$		
19	$\nu(C_8N_9)$	964	1037	38	$\gamma(invNH_2)$	156	214
	$\beta(N_9H)$				$\tau(R_3)$		
20	$\beta(roNH_2)$	921	1005		$\tau(R_r)$		
	$\nu(C_6N_3)$			39	$\tau(R_2)$	146	162
	$\nu(N_3C_2)$				$\tau(R_1)$		
21	$\gamma(C_2H)$	901	958		$\tau(R_3)$		
					$\gamma(C_6N_{10})$		

Comparison is made with experimental data from ref. 46.

Šponer,[34] for example, amount to 2.56, 6.49, 6.65, and 4.37 Debye for adenine, cytosine, guanine, and thymine, respectively. Similar values are also reported in ref. 51. It should be noted that the results from the quantum chemical calculations depend on the basis set used. The deviations can be as large as 0.3 Debye.[34,51]

Ionization Energies and Electron Affinities

The reliable determination of ionization energies and electron affinities of DNA bases is important in the context of understanding radiation-induced damage to the bases, which can alter the

Table 6. Calculated Dipole Moments in Each Direction (cf. Fig. 2 for the Axes Orientation) and Absolute Values (in Debye) of Adenine (A), Cytosine (C), Guanine (G), and Thymine (T) in Comparison with Experimental Data from Refs. 52–54.

	DFT-GGA				Exp.
	μ_x	μ_y	μ_z	μ	μ
A	−2.55	−0.29	0.00	2.56	2.5[a]
C	−5.51	−3.43	0.22	6.49	7.0[b]
G	5.33	−4.37	0.16	6.89	7.1[a]
T	0.53	−4.45	0.02	4.48	4.1[c]

[a]From ref. 53.
[b]From ref. 54.
[c]From ref. 52.

genetic code and may lead to the separation of entire DNA strands. The calculation of excited configurations within DFT-GGA, however, is complicated. On one hand, the calculations presented here refer to spin-averaged configurations. On the other hand, the density-functional theory by derivation only describes the electronic ground state correctly. Excitation energies calculated from the Kohn–Sham (KS) orbital energies of DFT are usually underestimated, due to the neglect of electronic self-energy effects.[9–11] If electrons are optically excited, in addition to the self-energy, the Coulomb attraction between electrons and holes also needs to be considered for calculations of realistic transition energies. For the delocalized electron gas, these effects are usually taken into account using a Green's function technique.[12,13,15,16,55]

In the present case, however, the localization of the electronic states allows for a numerically far less demanding treatment of these many-body effects: we investigate their influence by means of delta self-consistent field (ΔSCF)—also called constrained-DFT—calculations. Thereby the total-energy differences between the ground states and the excited states of the molecules are calculated. The electrons are allowed to relax, while the occupation numbers are constrained to the excited configuration. Here, we determine the lowest single-electron excitation, the ionization energy (IE)

$$\mathrm{IE} = E(N-1) - E(N), \tag{1}$$

and the electron affinity (EA)

$$\mathrm{EA} = E(N) - E(N+1), \tag{2}$$

where $E(N)$ denotes the ground-state energy of the molecule with N electrons. The ionized molecules with one missing or additional electron are characterized by the total energies $E(N-1)$ and $E(N+1)$, respectively. Using (1) and (2), the calculation of single-particle excitation energies reduces to the treatment of electronic ground states. In addition, structural relaxations can be taken into account. Then, instead of the vertical IEs and EAs, which include only electronic relaxation effects, one obtains adiabatic values.

Explicit calculations suffer from the limitations of the supercell approach. For that reason, we use monopole and dipole corrections[56,57] in ΔSCF calculations for charged systems, to compensate for the errors in the total-energy and forces induced by the spurious long-range interactions between neighboring supercells.

The vertical and adiabatic values of the IEs and EAs computed within the ΔSCF Schemes (1) and (2) are listed in Table 7. They are compared with the relative positions of the KS values for the highest occupied molecular orbitals (HOMO) and lowest unoccupied molecular orbitals (LUMO) with respect to the effective potential in the vacuum region of the supercell. The values obtained in this way are denoted by DFT-GGA. Table 7 indicates an effect of the structural relaxation on the IEs of about 0.1–0.2 eV. In contrast, this effect is negligible for the EAs. The additional electron in the LUMO state does not induce a noticeable change of the atomic geometry compared to the ground state.

More important are the electronic relaxation effects. With respect to the KS values (DFT-GGA) the IEs (EAs) are shifted towards larger (smaller) values by 2.6–3.0 eV (0.4–1.3 eV). In any case, the many-body effects beyond DFT-GGA increase the energetic distance between the single-particle excitations in the HOMO and LUMO states. Because we did not obtain fully converged results for thymine, EAs calculated within the ΔSCF method are only cited for adenin, cytosine, and guanine.

Experimentally, adiabatic IEs of 8.26, 8.68, 7.77, and 8.87 eV were determined for adenine, cytosine, guanine, and thymine.[58] These values agree within 0.2 eV with our calculations. An error bar of the same size has been found in earlier quantum chemistry calculations (cf. Table 1 in ref. 59). The comparison of the calculated vertical IEs with the experimental results of 8.44, 8.94, 8.24,

Table 7. Calculated Ionization Energies and Electron Affinities (in eV) of Adenine (A), Cytosine (C), Guanine (G), and Thymine (T).

	Ionization energies			Electron affinities		
	DFT-GGA	Vertical	Adiab.	DFT-GGA	Vertical	Adiab.
A	5.54	8.23	8.06	1.73	0.74	0.79
C	5.83	8.75	8.66	2.18	0.84	0.84
G	5.08	7.82	7.63	1.22	0.84	0.85
T	6.16	9.13	9.08	2.40		

and 9.14 eV for adenine, cytosine, guanine, and thymine[60] is of the same accuracy. Only the agreement for guanine is worse. There is quite a scatter in the theoretical values, ranging for guanine for example from 7.31 eV determined with ΔSCF B3LYP/6-31G* calculations[61] to 8.1 eV obtained using a semiempirical NDDO-G approach.[62] It is interesting to note that the same relative order of IEs G < A < C < T in agreement with experiment is obtained within all computational schemes applied in our study.

The single-particle DFT-GGA calculations predict the same order G < A < C < T for the sequence of the EAs. Within the ΔSCF calculations, however, the relative order changes and the affinities of guanine and cytosine get very close. Neither the single-particle nor the ΔSCF calculations, however, indicate nearly vanishing or negative EAs as found experimentally: Vertical EAs of −0.54, −0.32, and −0.29 eV are reported for adenine, cytosine, and thymine, respectively.[63] The corresponding adiabatic values amount to 0.012 ± 0.005,[64] 0.085 ± 0.008,[65] and 0.068 ± 0.020 eV.[64] These discrepancies may be related to the difficulty to model systems with negative EAs. Only stable bound states are readily accessible to the calculations, and for molecules with negative EAs no stable bound state exists. Correspondingly, in the literature there is a large scatter of calculated values. Negative or in some cases nearly vanishing EAs have been calculated in recent *ab initio*[59,66] and semiempirical calculations,[67] whereas B3P86 calculations by Wesolowski et al.[68] result in adiabatic EAs of 0.01, 0.54, 0.36, and 0.71 eV for adenine, guanine, cytosine and thymine, respectively.

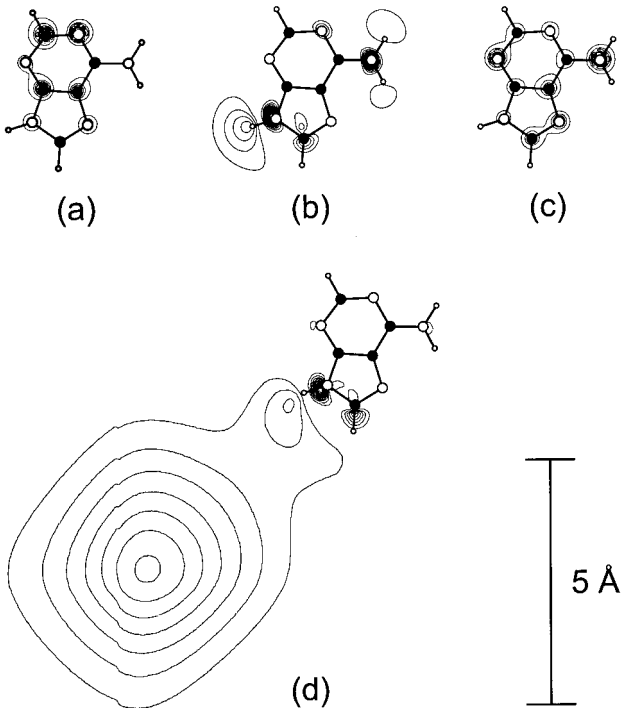

Figure 3. Contour plots of squared adenine wave functions in the molecular plane illustrating the HOMO/LUMO before (a/b) and after removal/addition of one electron (c/d). The contours are spaced by $4 \cdot 10^{-2}$, $1 \cdot 10^{-2}$ and $5 \cdot 10^{-3}$ Å^{-3} in (a/c), (b), and (d), respectively. Small empty (large empty, filled) circles represent hydrogen (nitrogen, carbon) atoms.

Table 8. HOMO-LUMO Pair Transition Energies (in eV) of Adenine (A), Cytosine (C), Guanine (G), and Thymine (T) Calculated in the Single-Particle Picture ($E^{ex}_{DFT\text{-}GGA}$), Including Electronic Relaxation, Self-Energy, and Electron-Hole Attraction Effects ($E^{ex}_{\Delta SCF}|_N$), and Including Additionally Structural Relaxation Effects ($E^{ex}_{\Delta SCF}|_{N,e+h}$).

	$E^{ex}_{DFT\text{-}GGA}$	$E^{ex}_{\Delta SCF}\|_N$	$E^{ex}_{\Delta SCF}\|_{N,e+h}$
A	3.84	3.95	3.77
C	3.64	4.03	3.70
G	3.85	4.01	3.32
T	3.76	3.95	3.58

A delocalized excess electron presents an obvious obstacle to an accurate ΔSCF calculation of the EA within the supercell approach. To illustrate the degree of delocalization, we plot in Figure 3 the orbital character of the adenine HOMO and LUMO, before and after one electron has been removed or added, respectively. As can be seen from the figure, upon electron removal and subsequent electronic relaxation, the HOMO changes its character to some extent. On the expense of the carbon atoms, the probability density is increased around most nitrogen atoms. Much more drastic changes, however, occur upon electron addition and subsequent relaxation of the LUMO. The orbital is partially smeared out in a region more than 5 Å away from the molecule. It extends over a large fraction of the supercell. Due to the periodic boundary conditions it is necessarily influenced by the neighboring images. Consequently, the electronic relaxation is not modeled correctly and the supercell ΔSCF calculation fails to account for the measured EA.

Pair Excitations

Similar to ionization energies and electron affinities, the lowest optical excitation energy may be calculated according to

$$E^{ex}_{\Delta SCF} = E(N, e + h) - E(N), \tag{3}$$

where $e + h$ indicates the presence of an electron-hole pair. Here, the calculation of the total energy $E(N, e + h)$ is done by applying the occupation constraint that the HOMO of the ground state system contains a hole and the excited electron resides in the LUMO of the ground-state system. This approach is exact within exact DFT.[69] If the exchange and correlation energy is approximated by using either the LDA or the GGA, the ΔSCF method works very well for localized electronic systems with a spatial extent below about 3 nm.[70] The energies can be calculated for the atomic geometry of the electronic ground state, $E^{ex}|_N$, or for the geometry in the presence of the electron-hole pair, $E^{ex}|_{N,e+h}$. They correspond to absorption or emission experiments. The difference $\Delta_{Stokes} = E^{ex}|_N - E^{ex}|_{N,e+h}$ gives the Stokes shift between absorption and luminescence lines.

HOMO-LUMO pair transition energies calculated according to this scheme are presented in Table 8. Values are listed for the

ground-state geometry, $E^{ex}_{\Delta SCF}|_N$, as well as for the relaxed geometries in the presence of an excited electron-hole pair, $E^{ex}_{\Delta SCF}|_{N,e+h}$. In addition, the simplest approximation to the transition energy is given, i.e., the difference of the single-particle KS eigenvalues, $E^{ex}_{DFT\text{-}GGA} = \varepsilon_{LUMO} - \varepsilon_{HOMO}$. The latter transition energies vary between about 3.6 eV for cytosine and 3.8 eV for guanine. They do not contain the contributions due to the relaxation of the molecular wave functions upon excitation, and neither electronic self-energy effects nor the attraction between electron and hole. These contributions are included by performing ΔSCF calculations according to expression (3) for $E^{ex}_{\Delta SCF}$.

We observe that the widening of the energy gaps due to the electronic self-energy is partially canceled by the gap narrowing due to the Coulomb attraction between electrons and holes and relaxation effects. The net effect consists in a small increase of the transition energies between about 0.1 eV for adenine and 0.4 eV for cytosine. Similar observations have been made for other confined systems such as Si and Ge nanocrystallites.[71] The resulting optical absorption energies amount to about 4 eV for all molecules considered (cf. Table 8).

The vertical IEs and EAs calculated using the ΔSCF method contain self-energy contributions, but no excitonic effects. Therefore, the differences between IEs and EAs reduced by the electronically relaxed HOMO-LUMO transition energies, $IE - EA - E^{ex}_{\Delta SCF}|_N$, correspond to the strength of the electron-hole attraction. Thus, we predict large exciton binding energies of 3.54, 3.88, and 2.97 eV for the HOMO-LUMO transitions of adenine, cytosine, and guanine, respectively.

As outlined before, the Stokes shift as the energy difference between absorption and luminescence lines can be calculated by taking into account the relaxation of the molecule geometry in the presence of the excited electron-hole pair in addition to the electronic relaxation. These shifts are considerable. The largest Stokes shift amounts to about 0.7 eV for guanine. Also, the difference between adiabatic and vertical IEs was found to be largest in this case, pointing out the strong influence of the HOMO occupation on the equilibrium geometry of guanine. In general, the structural relaxations due to the HOMO-LUMO excitation enlarge the molecules, due to the partial antibonding character of the LUMO. In the case of thymine and cytosine, for example, we find that, in particular, the carbon–carbon double bonds $C_5{=}C_6$ are affected. They are stretched by 0.11 and 0.08 Å, respectively. Also some contractions occur, however. That concerns for example the bond $C_4{-}C_5$, which is shortened by 0.04 Å for both thymine and cytosine. Our results for excited-state geometries are in good qualitative agreement with configuration interaction calculations by Shukla and Mishra[32] considering single-electron promotions.

Absorption Spectra

We also perform single-particle DFT-GGA and ΔSCF calculations to obtain the optical absorption spectra of adenine, guanine, cytosine, and thymine (cf. Fig. 4). These spectra are determined from all-electron wave functions obtained by the projector-augmented wave (PAW) method[72] and refer to zero-temperature calculations. The influence of the quantized vibrations and rotations at finite temperatures will considerably broaden the spectra, as will the interaction with solvent molecules. To identify qualitative trends, however, spectra such as presented here may still be useful. In calculating the ΔSCF spectra we use the oscillator strength obtained in the independent-particle approximation, i.e., the PAW matrix elements in DFT-GGA quality. However, the excitation energies are corrected for self-energy effects and electron-hole attraction according to the Scheme (3) with the appropriate occupation constraint.

Within the single-particle DFT-GGA calculations, the calculated onset of photon absorption occurs for all DNA bases for energies slightly below 4 eV, at the energy of the HOMO-LUMO transitions. The oscillator strengths of these transitions, as well as the absorption behavior for higher energies, however, are strongly molecule specific. Guanine and thymine are characterized by relatively few and energetically well separated (by about 1 eV) optical transitions, whereas the separation of the absorption peaks is much reduced in the cases of adenine and cytosine. As can be seen from the ΔSCF spectra, the influence of the many-body corrections on the absorption spectra is large and transition specific. The net effect consists in an increase of the excitation energy by one to several tenths of an eV for all DNA bases.

Due to the methodological limitations of our study such as the missing Coulomb enhancement of the oscillator strengths and the neglected coupling to the molecule vibrations, the comparison with previous calculations and experiment has to be made with caution. The fact that we predict optical transitions between the HOMO and LUMO states for all DNA bases seems to agree with earlier *ab initio* multireference configuration interaction calculations,[73] which predict four or even more transitions below 6.5 eV for the gas-phase nucleic acid bases. More recent findings by Fülscher et al.[74–76] are based on a quantum chemical multiconfigurational approach to describe the electronic excitations, the complete active space self-consistent field method (CASSCF). In the case of cytosine, they obtained 4.4, 5.4, 6.2, and 6.7 eV for the four lowest lying $\pi \rightarrow \pi^*$ transitions. This is in qualitative agreement with our ΔSCF transition energies of 4.79, 5.85, 6.08, and 6.85 eV, provided we discard the first peak at 4.03 eV, which has a relatively low oscillator strength. Measured peaks occur at 4.6–4.7, 5.2–5.8, 6.1–6.4, and 6.7–7.1 eV.[77] For adenine we find the most intense absorption at ΔSCF energies of 3.93, 4.71, 5.20, 5.69, 6.82, and 7.51 eV. Experiments[78–82] indicate the existence of transitions at 4.9, 5.7–6.1, 6.8, and 7.7 eV. Again, apart from the lowest peak, which is not observed experimentally, the other transition energies agree with an accuracy of better than 0.2 eV. However, our results cannot be unambiguously ascribed to the experimental values or to the results of Fülscher et al.,[75] because the occupied molecular orbitals do not have clearcut π-character, but consist additionally of carbon and nitrogen lone pairs that partially form σ-combinations. The same holds for guanine with ΔSCF transitions at 4.01, 4.62, 6.03, 6.29, 6.63, 7.00, and 8.32 eV (experimental values[78,83,84] at 4.5–4.8, 4.9–5.0, 5.5–5.8, 6.0–6.4, and 6.6–6.7 eV). Although lone-pair orbitals of σ-symmetry were included in the active space in Fülscher's calculations for guanine, orbital-type mixing was explicitely excluded. For thymine the correspondence between our calculated ΔSCF energies (4.10, 5.52, 6.73, 7.68 eV), the results of Fülscher et al.[76] (4.9, 5.9, 6.1, 7.1 eV), and experimental values[81–85] (4.5–4.7, 5.8–6.0, 6.3–6.6, 7.0 eV) seems to be better, possibly because the transitions we have obtained show a clearcut $\pi \rightarrow \pi^*$-character.

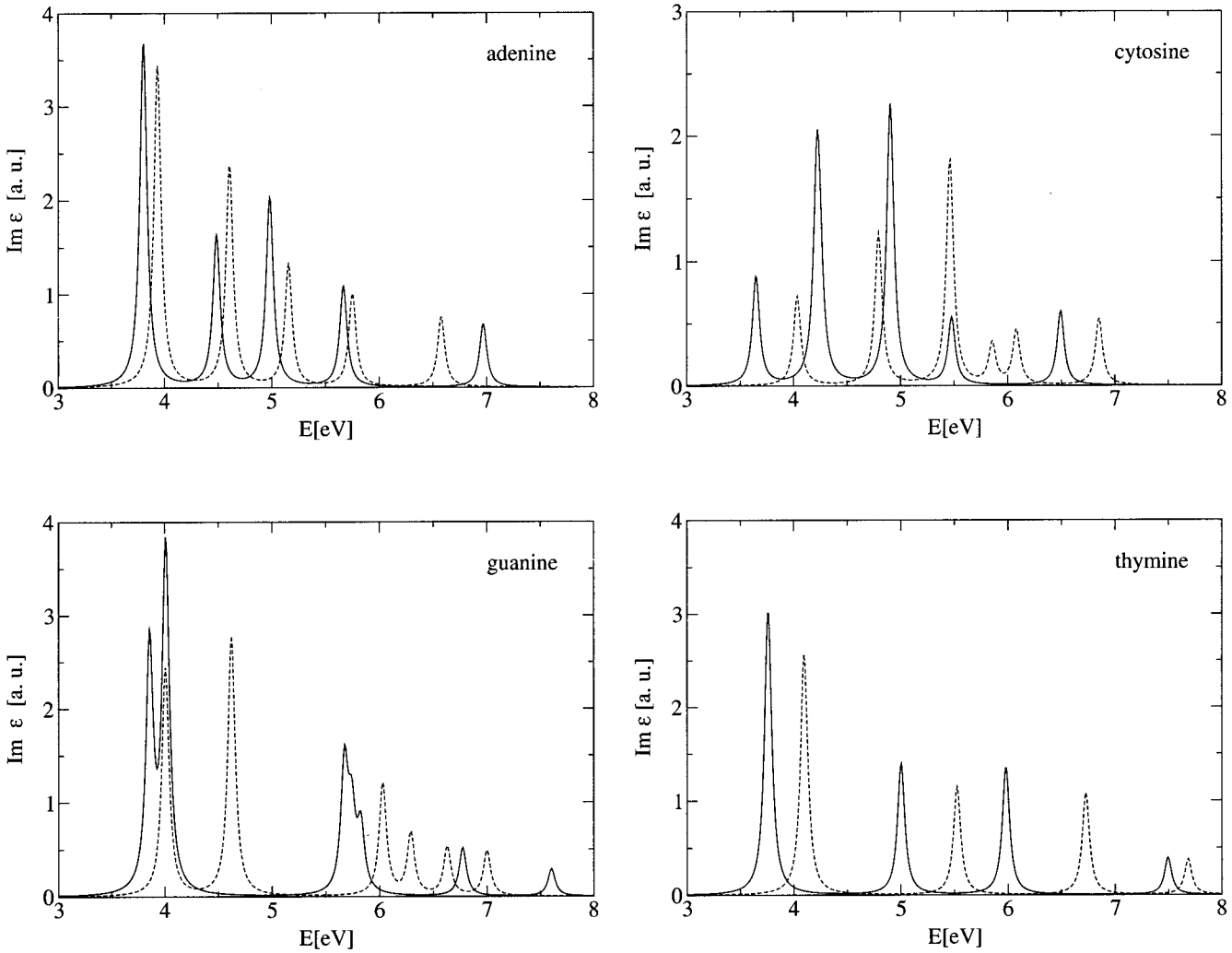

Figure 4. Imaginary part of the dielectric function calculated within DFT-GGA (solid lines) and the ΔSCF method (dashed lines) for the DNA bases.

Conclusions

The structural, vibrational, electronic, and optical properties of DNA bases have been calculated from first-principles using a DFT-GGA implementation based on ultrasoft pseudopotentials and a plane-wave basis set. The accuracy of the calculated bond lengths, vibrational frequencies, molecule dipoles, and ionization energies is comparable to *ab initio* quantum chemical methods. Our calculations result in a rather weak amino group pyramidalization for adenine, cytosine, and guanine. Pronounced differences between the optical absorption spectra of the DNA bases are observed, and large exciton binding energies between 3 and 4 eV are predicted for the HOMO-LUMO transitions.

Acknowledgments

Grants of computer time from the Leibniz-Rechenzentrum München, the Höchstleistungsrechenzentrum Stuttgart, and the John von Neumann-Institut Jülich are gratefully acknowledged.

References

1. Starikov, E. B. Int J Quantum Chem 2000, 77, 859.
2. Šponer, J.; Leszczynski, J.; Hobza, P. Biopolymers 2002, 61, 3.
3. Sühnel, J. Biopolymers 2002, 61, 32.
4. Boys, S. F.; Bernardi, F. Mol Phys 1970, 19, 553.
5. Hamza, A.; Vibok, A.; Halasz, G. J.; Mayer, I. J Mol Struct (Theochem) 2000, 501, 427.
6. Perdew, J. P.; Zunger, A. Phys Rev B 1981, 23, 5048.
7. Perdew, J. P.; Chevary, J. A.; Vosko, S. H.; Jackson, K. A.; Pederson, M. R.; Singh, D. J.; Fiolhais, C. Phys Rev B 1992, 46, 6671.
8. Perdew, J. P.; Burke, K.; Enzerhof, M. Phys Rev Lett 1996, 77, 3865.
9. Bechstedt, F. In Festkörperprobleme/Advances in Solid State Physics; Rössler, U., Ed.; Vieweg: Braunschweig/Wiesbaden, 1992, p. 161, vol. 32.
10. Aryasetiawan, F.; Gunnarsson, O. Rep Prog Phys 1998, 61, 237.
11. Aulbur, W. G.; Jonsson, L.; Wilkins, J. W. Solid State Physics: Advances in Research and Applications; Academic: San Diego, 2000, p. 1, vol. 54.

12. Albrecht, S.; Reining, L.; Del Sole, R.; Onida, G. Phys Rev Lett 1998, 80, 4510.
13. Benedict, L. X.; Shirley, E. L.; Bohn, R. B. Phys Rev Lett 1998, 80, 4514.
14. Rohlfing, M.; Louie, S. G. Phys Rev Lett 1998, 81, 2312.
15. Hahn, P. H.; Schmidt, W. G.; Bechstedt, F. Phys Rev Lett 2002, 88, 016402.
16. Schmidt, W. G.; Glutsch, S.; Hahn, P. H.; Bechstedt, F. Phys Rev B 2003, 67, 085307.
17. Vasiliev, I.; Ögüt, S.; Chelikowsky, J. R. Phys Rev B 1999, 81, 4959.
18. Onida, G.; Reining, L.; Rubio, A. Rev Mod Phys 2002, 74, 601.
19. Fellers, R. S.; Barsky, D.; Gygi, F.; Colvin, M. Chem Phys Lett 1999, 312, 548.
20. Di Felice, R.; Calzolari, A.; Molinari, E.; Garbesi, A. Phys Rev B 2001, 65, 045104.
21. Gervasio, F. L.; Carloni, P.; Parrinello, M. Phys Rev Lett 2002, 89, 108102.
22. Furthmüller, J.; Käckell, P.; Bechstedt, F.; Kresse, G. Phys Rev B 2000, 61, 4576.
23. Kresse, G.; Furthmüller, J. Comp Mater Sci 1996, 6, 15.
24. Ramos, L. E.; Furthmüller, J.; Bechstedt, F.; Scolfaro, L. M. R.; Leite, J. R. Phys Rev B 2002, 66, 075209.
25. Kohn, W. Rev Mod Phys 1999, 71, 1253.
26. Pulay, P. Chem Phys Lett 1980, 73, 393.
27. Wood, D. M.; Zunger, A. J Phys A 1985, 18, 1343.
28. Clowney, L.; Jain, S. C.; Srinivasan, A. R.; Westbrook, J.; Olson, W. K.; Berman, H. M. J Am Chem Soc 1996, 118, 509.
29. Fuchs, M.; Scheffler, M. Phys Rev B 1998, 57, 2134.
30. Podolyan, Y.; Rubin, Y. V.; Leszczynski, J. J Phys Chem A 2000, 104, 9964.
31. Šponer, J.; Hobza, P. J Phys Chem 1994, 98, 3161.
32. Shukla, M. K.; Mishra, P. C. Chem Phys 1999, 240, 319.
33. Gu, J. D.; Leszczynski, J. J Phys Chem A 1999, 103, 2744.
34. Hobza, P.; Šponer, J. Chem Rev 1999, 99, 3247.
35. Šponer, J.; Hobza, P. Int J Quantum Chem 1996, 57, 959.
36. Leszynski, J. Int J Quantum Chem 1992, 43, 19.
37. Šponer, J.; Leszczynski, J.; Hobza, P. J Biomol Struct Dyn 1996, 14, 117.
38. Kwiatkowski, J. S.; Leszczynski, J. J Phys Chem 1996, 100, 941.
39. Estrin, D. A.; Paglieri, L.; Corongu, G. J Phys Chem 1994, 98, 5653.
40. Smets, J.; Adamowicz, L.; Maes, G. J Phys Chem 1996, 100, 6434.
41. Bludský, O.; Šponer, J.; Leszcynski, J.; Špirko, V.; Hobza, P. J Chem Phys 1996, 105, 11042.
42. Kress, C.; Fiedler, M.; Schmidt, W. G.; Bechstedt, F. Phys Rev B 1994, 50, 17697.
43. Bechstedt, F.; Stekolnikov, A.; Furthmüller, J.; Käckell, P. Phys Rev Lett 2001, 87, 016103.
44. Lister, D. G.; Tyler, J. K.; Høg, J. H.; Larsen, N. W. J Mol Struct 1974, 23, 253.
45. Schmidt, W. G.; Bechstedt, F.; Srivastava, G. P. Phys Rev B 1995, 52, 2001.
46. Nowak, M. J.; Lapinski, L.; Kwiatkowski, J. S.; Leszczynski, J. J Phys Chem 1996, 100, 3527.
47. Szczesniak, M.; Szczepaniak, K.; Kwiatkowski, J. S.; KuBulat, K.; Person, W. B. J Am Chem Soc 1988, 110, 8319.
48. Fritsch, J.; Pavone, P.; Schröter, U. Phys Rev Lett 1993, 71, 4194.
49. McCarthy, W. J.; Lapinski, L.; Nowak, M. J.; Adamowicz, L. J Chem Phys 1995, 103, 656.
50. Podolyan, Y.; Rubin, Y. V.; Leszczynski, J. Int J Quantum Chem 2001, 83, 203.
51. Li, J. B.; Xing, J. H.; Cramer, C. J.; Truhlar, D. G. J Chem Phys 1999, 111, 885.
52. Kulakowski, I.; Geller, M.; Lesyng, B.; Wierzcho, K. L. Biochim Biophys Acta 1974, 361, 119.
53. DeVoe, H.; Tinoco, I., Jr. J Mol Biol 1962, 4, 500.
54. Weber, H.-P.; Craven, B. M. Acta Crystallogr 1990, B46, 532.
55. Rohlfing, M.; Louie, S. G. Phys Rev Lett 1998, 80, 3320.
56. Makov, G.; Payne, M. C. Phys Rev B 1995, 51, 4014.
57. Neugebauer, J.; Scheffler, M. Phys Rev B 1992, 46, 16067.
58. Orlov, V. M.; Smirnov, A. N.; Varshavsky, Y. M. Tetrahedron Lett 1976, 48, 4377.
59. Russo, N.; Toscano, M.; Grand, A. J Comput Chem 2000, 21, 1243.
60. Hush, N. S.; Cheung, A. S. Chem Phys Lett 1975, 34, 11.
61. Prat, F.; Houk, K. N.; Foote, C. S. J Am Chem Soc 1998, 120, 845.
62. Voityuk, A. A.; Jortner, J.; Bixon, M.; Rösch, N. Chem Phys Lett 2000, 324, 430.
63. Aflatooni, K.; Gallup, G. A.; Burrow, P. D. J Phys Chem A 1998, 102, 6205.
64. Desfrancois, C.; Abdoul-Carime, H.; Schermann, J. P. J Chem Phys 1996, 102, 1274.
65. Schiedt, J.; Weinkauf, R.; Neumark, D. M.; Schlag, E. W. Chem Phys 1998, 239, 511.
66. Li, X.; Cai, Z. J Phys Chem 2002, 106, 1596.
67. Voityuk, A. A.; Michel-Beyerle, M.-E.; Rösch, N. Chem Phys Lett 2000, 342, 231.
68. Wesolowski, S. S.; Leininger, M. L.; Pentchev, P. N.; Schaefer, H. F. J Am Chem Soc 2001, 123, 4023.
69. Sham, L. J.; Schlüter, M. Phys Rev Lett 1983, 51, 1888.
70. Godby, R.; White, I. D. Phys Rev Lett 1998, 80, 3161.
71. Weissker, H. C.; Furthmüller, J.; Bechstedt, F. Phys Rev Lett 2003, 90, 085501.
72. Adolph, B.; Furthmüller, J.; Bechstedt, F. Phys Rev B 2001, 63, 125108.
73. Jensen, H. J. A.; Koch, H.; Jørgensen, P.; Olsen, J. J Chem Phys 1988, 119, 297.
74. Fülscher, M. P.; Roos, B. O. J Am Chem Soc 1995, 117, 2089.
75. Fülscher, M. P.; Serrano-Andrés, L.; Roos, B. O. J Am Chem Soc 1997, 119, 6168.
76. Lorentzon, J.; Fülscher, M. P.; Roos, B. O. J Am Chem Soc 1995, 117, 9265.
77. Callis, P. R. Annu Rev Phys Chem 1983, 34, 329.
78. Sprecher, C. A.; Johnsen, W. C., Jr. Biopolymers 1977, 16, 2243.
79. Brunner, W. C.; Maestre, M. F. Biopolymers 1975, 14, 555.
80. Miles, D. W.; Hahn, S. J.; Robins, R. K.; Eyring, H. J Phys Chem 1967, 72, 1483.
81. Yamada, T.; Fukutome, H. Biopolymers 1968, 6, 43.
82. Clark, L. B.; Peschel, G. G.; Tinoco, I., Jr. J Phys Chem 1965, 69, 3615.
83. Voelter, W.; Records, R.; Bunnenberg, E.; Djerassi, C. J Am Chem Soc 1968, 90, 6163.
84. Voet, D.; Gratzer, W. B.; Cox, R. A.; Doty, P. Biopolymers 1963, 1, 193.
85. Clark, L. B.; Tinoco, I., Jr. J Am Chem Soc 1965, 87, 11.